

1 Theoretical Aspects of Nuclear Shielding

A. Ab Initio Calculations.- Nuclear shieldings of Cu, Ag, Zn, Cd, and Mn in metal complexes were calculated by a finite perturbation SCF method using the MIDI-1 basis set for metal atoms and ligands.^{1,2} This basis set is of double zeta quality for valence orbitals. The gauge origin is taken at the position of the metal atom. In these complexes the primitive metal atoms are characterized by the ground state electronic configuration $d^{10}s^1-2p^0$ except for Mn which is d^5s^2 . The complexes studied are $Ag(H_2O)_6^+$, AgF_4^{3-} , $AgCl_2^-$, $AgCl_4^{3-}$, $Ag(CN)_4^{3-}$, $Ag(NH_3)_2^+$, $Cd(H_2O)_6^{2+}$, $CdCl_2$, $CdCl_4^{2-}$, $Cd(CN)_4^{2-}$, $Cd(CH_3)_2$, $CuCl$, $CuCl_4^{3-}$, $Cu(CN)_4^{3-}$, $Cu(NH_3)_2^+$, $Zn(H_2O)_6^{2+}$, $ZnCl_2$, $ZnCl_4^{2-}$, $Zn(CN)_4^{2-}$, $Zn(NH_3)_4^{2+}$, and $Mn(CO)_5L$ ($L = H, CN, CH_3, Cl$). The shielding contributions are analyzed according to diamagnetic and paramagnetic contributions and in terms of individual MO contributions to each. As expected, the ligand AOs make only minor contributions to the metal shielding. For example, in $Cd(CH_3)_2$ only 75/4851 of the diamagnetic term and -29/1090 of the paramagnetic term come from the two CH_3 ligands. The diamagnetic term is dominated by the inner core MOs on the metal, the valence MO contributions are only 5-18% of the total diamagnetic term. Although the absolute shielding is dominated by the diamagnetic term, the differences in shielding between molecules are primarily determined by the valence MO contributions to the paramagnetic term. These findings support the general assumptions which are usually invoked in approximate treatments of chemical shifts which include only the valence MO contributions to the paramagnetic term. The small changes in the diamagnetic term from one complex to another result from the transferability of the core MOs and the small relative contributions of ligand orbitals.

The calculated metal d orbital versus p orbital contributions to shielding are described qualitatively in terms of the empirical electron donating and withdrawing properties of the ligand. For the $d^{10}s^1-2p^0$ configuration, an electron-donating ligand deshields the metal nucleus primarily by donation of electrons from the ligands to the metal p orbitals whereas an electron-withdrawing ligand deshields the metal nucleus via back-donation of electrons from the metal d orbitals to the ligands. The relative contributions of the d and p mechanisms depend on the metal and the number and nature of the ligands.

The calculations on the Mn complexes as representative transition metal compounds show that the paramagnetic term and the chemical shifts between complexes arise primarily from terms, which in the perturbation scheme, are represented by transitions which are largely $d_{\pi} \rightarrow d_{\sigma}$. This explains why approximate treatments which consider only the $d_{\pi} \rightarrow d_{\sigma}$ terms using a simple crystal field model work at all. The paramagnetic contribution to the shielding in Mn is an order of magnitude larger than those of the IB and IIB metal complexes. In the former there is a paramagnetic shielding which arises due to an intrinsic open d shell, whereas in the latter, mechanisms of electron donation to or from ligands are necessary in order to create holes in the d shell or electrons in the outer p shell of the metal atom.

For nuclear sites of sufficiently low symmetry there are non-vanishing off-diagonal shielding components $\sigma_{ij}(j \neq i)$ in the principal axis system, reviewed in the previous volume of this series. The antisymmetric components of the ^{13}C shielding tensor³ in several compounds (oxetane, cyclopentane, 1,3-cyclopentadiene, 1,4 cyclohexadiene, nitromethane, acetone, acetaldehyde, cyclopentane, ethylene sulfide, ethylene oxide, cyclopropene, and cyclobutene) have been calculated using the individual gauge for localized orbitals (IGLO) method.⁴ The root mean square antisymmetric components $[\sum_{i,j=1}^3 (\sigma_{ij}^a)^2]^{1/2}$ range from 1.0 ppm in $\text{CH}_3^{13}\text{CHO}$ to 139.4 ppm in cyclopropene ($^{13}\text{C}=\text{C}$). The contribution of the antisymmetric components of the shielding to spin-lattice relaxation by shielding interactions can be large enough in some cases (0.20 to 0.88 times as large as the shielding anisotropy contribution, and 2.0 times as large in the cyclopropene case), to be a significant contributor to this relaxation mechanism. Nevertheless, the experimental determi-

nation of the sum of the squares of the antisymmetric shielding components is problematical unless the shielding interactions mechanism can be made dominant by observing favorable molecules in very high fields. Nuclei much heavier than ^{13}C should be more favorable. Unfortunately, the antisymmetric components of the shielding are less accurately estimated in these cases and the results now available from this work,⁴ and those reviewed in the previous volume of this series,⁵ do not show any obvious correlations between electronic structure and magnitudes of ^{13}C antisymmetric components.

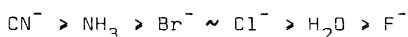
Calculations of ^1H and ^{13}C shielding in a variety of small molecules (CH_4 , CH_3NH_2 , CH_3OH , CH_3F , CH_2F_2 , CHF_3 , CF_4 , HCN , H_2CO , C_2H_6 , C_2H_4 , C_2H_2 , CH_3CHO , $\text{CH}_3\text{CH}_2\text{CH}_3$, $\text{CH}_3\text{CH}=\text{CH}_2$, $\text{CH}_2=\text{C}=\text{CH}_2$, $\text{CH}_3\text{C}\equiv\text{CH}$, NH_3 , H_2O , HF) by Ditchfield's GIAO SCF FPT method using 4-31G basis sets give relative proton shifts to ± 0.5 ppm and relative ^{13}C shifts to ± 6 ppm compared to gas-phase data.⁶ The calculated absolute shieldings tend to be too shielded compared to experiment. Of course, some of the discrepancy can be accounted for by rovibrational corrections, but for tetrahedral carbons these tend to be small. For CH_4 for example, it is estimated to be -3.3 ppm. SOS-CI calculations of ^1H and ^{17}O shielding in H_2O_2 using a 6-31G** basis set give $\sigma(^1\text{H}) = 22.24$ ppm, which is 7.8 ppm less shielded than ^1H in H_2O by a similar calculation, $\sigma(^{17}\text{O}) = 149.5$ ppm which is 146.7 ppm less shielded than the calculated ^{17}O in H_2O , which in turn is about 50 ppm too deshielded compared to experiment.⁷ The ^1H shieldings in isolated H_2O , H_3O^+ , and OH^- , respectively are 31.2, 22.2, and 39.1 ppm at the equilibrium configuration. The ^{17}O shieldings are 326.5, 298.9, 318.0 ppm respectively.⁸ In this calculation the ^{17}O shielding in H_2O is also too deshielded compared to the experimental value of 357 ± 17 ppm, which is obtained from the absolute shielding scale recently reported by Wasylishen⁹ based on the molecular beam experiment on C^{17}O . The gas phase value for H_2O is 344.0 ppm at 293 K, which when combined with the 13.6 ppm vibrational correction by Fowler and Raynes¹⁰ gives $\sigma_{\text{e}}(^{17}\text{O} \text{ in } \text{H}_2\text{O}) = 357$ ppm. The available ^{17}O shielding calculations for H_2O (reviewed in Vol. 12 of this series) also give results which are less shielded than experiment. Apparently, the paramagnetic contribution to ^{17}O shielding is overestimated by theoretical calculations.⁹

B. Semi-empirical Calculations.- An empirical relation between two experimentally independent quantities: the chemical shift on the one hand and an optical parameter which can be calculated from the visible-UV spectrum of the complex on the other hand has been presented.¹¹ For d^6 complexes such as those of Co(III) the optical parameter incorporates the nephelauxetic ratio ($\beta = B_{\text{complex}}/B_{\text{gaseous ion}}$, the ratio of the Racah parameters for interelectronic repulsion) which is calculated together with the L matrix elements, within the framework of the parametrized d^6 model on the basis of the two absorption bands of cubic parentage for the complex. The energies of the first and second cubic transitions are predominantly determined by β . Thus, a parameter Σ is defined:

$$\Sigma(\alpha) = h_1(a^1T_{1g}(\alpha))/\beta \quad (1)$$

where $h_1(a^1T_{1g}(\alpha))$, $\alpha = x, y, z$ is the energy of the first cubic transition $a^1A_{1g} + a^1T_{1g}$ as obtained from the visible-UV spectrum. The a in front of the term symbol indicates that this is the lowest term of the symmetry type in question. $h_2(a^1T_{2g}(\alpha))$ corresponds to the $a^1A_{1g} + a^1T_{2g}$ transition.

In the interpretation of chemical shifts of d^6 complexes both the spectrochemical series (Δ series) of ligands and the nephelauxetic series (β series) have been used. The present observation indicates that the order of transition metal chemical shifts induced by ligands might be governed by an "internal field strength" parameter Δ/B . The internal field strength series for ligands runs as



in which the heavy halides have been moved forward with respect to the spectrochemical series due to their high nephelauxetism (low B values). The dimensionless internal field strength parameter Δ/B is empirically determined from those values of Δ and B which reproduce the observed transition energies h_1 and h_2 as differences between the lowest eigenvalues of the $A_{1g}(5 \times 5)$, $T_{1g}(4 \times 4)$, and $T_{2g}(7 \times 7)$ matrices for the energies in an intermediate field (in which the off-diagonal elements represent the interelectronic repulsion). In the interval $1.10 < h_2/h_1 < 1.55$, Δ and B can be approximately described by a numerical fit:

$$\Delta = h_1 + (h_2 - h_1) * \{0.1824(h_2/h_1)^2 - 0.5531(h_2/h_1) + 0.6165\}.$$

$$\beta = (h_2 - h_1) * \{4.077 \times 10^{-2}(h_2/h_1)^2 - 7.090 \times 10^{-2}(h_2/h_1) + 9.352 \times 10^{-2}\}. \quad (2)$$

The paramagnetic term is then written in terms of the parameters $\Sigma^{(\alpha)}$, $\alpha = x, y, z$ and $(\langle r_{3d}^{-3} \rangle / \beta)$:

$$\sigma^p = -(\mu_0 e^2 / 12 \pi m^2) (\langle r_{3d}^{-3} \rangle / \beta) \cdot \left\{ \sum_{\alpha=x,y,z} \left| \langle a^1 A_{1g} | L_{\alpha} | a^1 T_{1g}^{(\alpha)} \rangle \right|^2 / \Sigma^{(\alpha)} \right\}. \quad (3)$$

This gives an improved linear correlation for ^{59}Co shifts in Co(III) complexes and the slope of the straight line reflects the magnitude of the unknown parameter $(\langle r_{3d}^{-3} \rangle / \beta)$. This "effective" r^{-3} value includes the influence of the ligands on the radial term, if β is small, and nephelauxetism (electron cloud expansion) is large.

The conformation dependence of the ^{13}C chemical shifts has been calculated for carbonyl, C_{α} , and C_{β} in polyglycine I and II and poly(L-alanine) α -helix and β -sheet forms.¹² The results are found to be qualitatively consistent with the observed conformational dependence as determined by the cross-polarization MAS technique. ^{19}F chemical shifts in $\text{BF}_{4-n}(\text{OH})_n^-$ and $\text{BF}_{4-n}(\text{OOH})_n^-$ were calculated and discussed in terms of the electronic structure of these molecules.¹³

2 Physical Aspects of Nuclear Shielding

A. Anisotropy of the Shielding Tensor.— The ^{13}C shielding tensors in linear and pseudolinear (containing only H atoms off a C_{∞} axis) molecules have been determined by cross-polarization and intermolecular cross-polarization experiments on solid solutions of the molecule of interest in argon.¹⁴ The results are shown in Table 1 as absolute shielding, the reported chemical shifts relative to external liquid TMS were converted using an absolute shielding for TMS = 185.4 ppm.^{15,16} There are several interesting points worth noting in this study. One is that the assignments of three principal values to three principal axes in Table 2 required the correct relative ordering provided by theoretical calculations. The results of such calculations by a coupled Hartree-Fock method using individual gauges for localized molecular orbitals (IGLO) are also

reported.¹⁴ The calculated values of the components relative to CH₄ differ by less than 40 ppm from experiment, except in CO. Agreement with σ_{av} was much better (to within 17 ppm). The calculations agree with only one permutation of the experimentally

Table 1. Axially symmetric ¹³C absolute shielding tensor components, in ppm.¹⁴ Experimental values originally reported as ppm from TMS have been converted to absolute shielding values based on ¹³C in CO = 3.20±0.27 ppm.¹⁶ On this shielding scale ¹³C in liquid TMS at room temperature is 185.4 ppm.¹⁵

Molecule	σ_{\perp}	σ_{\parallel}	σ_{av}	$\sigma_{iso}(liq)$
CO	-119.6	233.4	-1.9	3.2
CO ₂	-59.6	275.4	52.1	53.2
OCS	-89.6	275.4	32.1	31.4
CS ₂	-146.6	277.4	-5.3	-7.4
C \equiv C \equiv C \equiv C=O	-49.6	275.4	58.7	57.7
O=C \equiv C \equiv C=O	161.4	275.4	199.4	200.0
HC \equiv CH	35.4	275.4	115.4	113.5
CH ₃ C \equiv CH	45.4	259.4	116.7	117.0
CH ₃ C \equiv CH	19.4	278.4	105.7	105.6
CH ₃ C \equiv CCH ₃	33.4	260.4	109.1	110.6
CH ₂ =C=CH ₂	-47.6	10.4	-28.3	-28.1

Table 2. ¹³C absolute shielding tensors, ppm,¹⁴ as in Table 1.

(\parallel) The component along the long axis of the molecule

(\perp) The component along an axis perpendicular to the long axis of the molecule, lying in the CH₂ plane.

Molecule	σ_{11}	σ_{22}	σ_{33}	σ_{av}	$\sigma_{iso}(liq)$
CH ₂ =CH ₂	-48.6(\perp)	65.4(\parallel)	161.4	59.4	62.1
CH ₂ =C=O	-79.6(\perp)	-53.6	108.4(\parallel)	-8.3	-8.6
*CH ₂ =C=O	146.4(\perp)	181.4	212.4(\parallel)	182.4	182.9
*CH ₂ =C=C*H ₂	27.4(\perp)	131.4(\parallel)	162.4	107.1	110.6

observed shielding components, thus allowing assignments with confidence. In linear molecules the paramagnetic contribution to σ is zero by symmetry so long as the gauge origin is chosen anywhere

along the line of centers. The similarity of the σ_z values in the linear molecules shows that the diamagnetic contribution varies only slightly from one electronic environment to another. With the presence of symmetry-breaking protons off-axis, the paramagnetic term is no longer "quenched" and contributes to the component along the long axis of the molecule in dramatic contrast to the linear case.

^{13}C shielding tensors have also been reported in quinol,¹⁷ HCN,¹⁸ halobenzenes, PhX (X = F, Cl, Br, I),¹⁹ in trans-polyacetylene,²⁰ and in L-asparagine monohydrate.²¹ In quinol and the halobenzenes, the component perpendicular to the molecular plane is the most shielded component and becomes more shielded with separation of the C atom from the substituent (with the exception of PhI), e.g., increasing from 91.4 ppm for the C_1 carbon to 185.4 ppm for the para carbon in PhF.¹⁹ In contrast the isotropic average does not show regular changes with the position of C in the ring. On the other hand, the shielding component of C_1 perpendicular to the ring changes drastically with X: 179.2 ppm in benzene (H), 173.4 ppm (I), 133.4 ppm (Br), 131.4 ppm (Cl), 118.4 ppm (OH), 91.4 ppm (F), in the direction one might expect by using electronegativity arguments. In HCN the ^{13}C shielding anisotropy is reported as 334 ± 20 ppm, and there is some indication that the molecular structure of HCN varies with liquid crystal solvents.¹⁸ The orientation of the ^{13}C shielding tensor axes in pairwise ^{13}C -enriched undoped trans-polyacetylene has been determined. $\sigma_{11} = -31.6$ ppm along an axis which makes an angle of $40 \pm 5^\circ$ with respect to the C-C bond and $80 \pm 5^\circ$ with the C=C bond. $\sigma_{22} = 42.4$ ppm, $\sigma_{33} = 140.4$ ppm along an axis perpendicular to the molecular plane.²⁰ A review of the anisotropy of ^{13}C shielding has been published.²²

The ^{15}N shielding tensor for the peptide bond in glycyglycine hydrochloride monohydrate has been reported.²³ The ^{17}O shielding tensors in the hexacarbonyls of Cr, Mo, and W are shown in Table 3.²⁴ The ^{13}C shielding tensors in the same molecules were measured as well, however the recent values do not differ significantly from the earlier report in Volume 11 of this series. ^{19}F nmr of single crystal sym- $\text{C}_5\text{Cl}_3\text{F}_3$ yields the following absolute shielding components: $\frac{1}{2}(\sigma_{11} + \sigma_{22}) = 262.8$ ppm, $\sigma_{33} = 390.8$ ppm, which may be compared to C_6F_6 in which they are 302.8 and 460.8 ppm respectively.²⁵ The ^{19}F powder spectrum at 77 K in CFBr_3 gives an anisotropy-

py $\Delta\sigma = 142 \pm 12$ ppm,²⁶ which is comparable to that in CFCl_3 . In KZnF_3 the ^{19}F nucleus is in a nearly ionic bond so the anisotropy is very small (18.6 ppm), $\sigma_{\parallel} = 390$ ppm and $\sigma_{\perp} = 371.4$ ppm, where the unique axis is along the Zn-F-Zn direction.²⁷

Table 3 ^{17}O absolute shielding tensor components, ppm.²⁴ The values originally reported in ppm relative to liquid H_2O are converted to absolute shielding using the new ^{17}O absolute shielding scale in which $\sigma(^{17}\text{O}$ in liquid $\text{H}_2\text{O}) = 307.9$ ppm based on ^{17}O in CO (molecular beam) = -42.3 ± 17.2 ppm.⁹

	σ_{11}	σ_{22}	σ_{33}	$\Delta\sigma$	σ_{av}
free CO	-142	-142	411	553	-42.3
$\text{Cr}(\text{CO})_6$	-307	-271	402	691	-58.8
$\text{Mo}(\text{CO})_6$	-277	-248	387	650	-46.1
$\text{W}(\text{CO})_6$	-259	-228	375	619	-37.4

Table 4 ^{31}P absolute shielding tensor components, in ppm.²⁹ The values originally reported in ppm relative to 85% H_3PO_4 are converted to absolute shielding using $\sigma(^{31}\text{P}$ in 85% $\text{H}_3\text{PO}_4) = 356$ ppm,³⁰ based on $\text{PH}_3 = 597$ ppm from the molecular beam results.³¹

	σ_{11}	σ_{22}	σ_{33}	$\Delta\sigma = \sigma_{\parallel} - \sigma_{\perp}$	σ_{av}
Free PO_4^{3-} (85% H_3PO_4)	356	356	356	0	356
End PO_4^{3-}					
$\text{K}_4\text{P}_2\text{O}_7$	274	399	399	-125	357.3
$\text{Na}_4\text{P}_2\text{O}_7$	276	393	393	-117	354
$\text{K}_5\text{P}_3\text{O}_{10}$	250	411	411	-161	357.3
$\text{K}_5\text{P}_3\text{O}_{10}$	266	407	407	-141	360
$(\text{NaPO}_3)_n$	261	401	401	-140	354
Branching PO_4^{3-}					
P_4O_{10}	290	321	596	290	402.3
in silica	319	319	546	227	394.7
Middle PO_4^{3-}					
$\text{K}_5\text{P}_3\text{O}_{10}$	281	340	504		375
$(\text{NaPO}_3)_n$	266	343	516		375

The ^{31}P shielding anisotropies in isolated, end, middle, and branching phosphate groups are related to the bond orders of the P-O bonds around the P nucleus.²⁹ The ideal PO_4^{3-} tetrahedron, an isolated phosphate ion, has 4 equal P-O_t bonds each with a bond order $\sim 5/4$ and an isotropic ^{31}P shielding. An end PO_4^{3-} and a branching PO_4^{3-} are axially symmetric PO_4^{3-} environments which can be considered as evolving from the isotropic PO_4^{3-} by transfer of π bond character from one bond to the other 3 bonds making 3 terminal P-O_t bonds and one P-O_b bridging bond (this is an end PO_4^{3-} moiety) or by transfer of π bond character from 3 bonds in the isotropic case to one bond, making one terminal P-O_t bond and 3 P-O_b bridging bonds (this is a branching PO_4^{3-} moiety). In the end phosphate groups the P-O_b along the symmetry axis has lost π bond character to the other 3 and this is accompanied by a decrease of ^{31}P shielding parallel to the axis and an increase perpendicular to this axis. A branching PO_4^{3-} , formed by transfer of π bond character to one P-O_t bond on the symmetry axis (a change of electron density in an opposite direction from that in the end phosphate group), has the opposite shielding anisotropy. The ^{31}P shielding parallel to the symmetry axis increases and shielding perpendicular to the axis decreases relative to the free PO_4^{3-} ion. In both the branching and end phosphates the change in shielding component parallel to the bond is in the same direction as the change in the bond order, whereas the component perpendicular to it changes in an opposite way. These effects are illustrated in Table 4. These results are in agreement with earlier data reviewed in Vol. 14 of this series. The shielding tensors of all three ^{31}P nuclei in chlorotris(triphenylphosphine) rhodium(I) are reported.³² The most shielded component is parallel to the P-Rh bond in each case.

^{29}Si shielding in single crystal Mg_2SiO_4 has the following shielding components: $\sigma_{11} = 38.8$ ppm, $\sigma_{22} = 55.3$ ppm, $\sigma_{33} = 95.4$ ppm relative to external TMS liquid.²⁸ ^{113}Cd tensors in Cd(II) acetate dihydrate, diacetate dihydrate, maleate dihydrate, formate dihydrate and diethylphosphate single crystals are reported.³³⁻³⁵ ^{119}Sn in $n\text{-Bu}_3\text{SnF}$ has shielding components of 157 ppm, 69 ppm, and -198 ppm relative to SnMe_4 .³⁶

B. The Effects of Rotation and Vibration.- The temperature dependence observed in the gas phase in the zero-pressure limit has been

interpreted in terms of the existence of a nuclear magnetic shielding surface which together with the intramolecular potential energy surface determines the rovibrationally averaged values of the shielding. The latter are measured as the residual shifts of the resonance frequencies with temperature after the intermolecular (density-dependent) effects have been removed. The same theoretical interpretation is used for the isotope shifts, measured as differences in resonance frequency between isotopomers, in which the isotopically substituted atom is one or more bonds away from the observed nucleus. The temperature dependence of the shielding in the isolated molecule is then expressed as

$$\sigma_0(T) = \langle \sigma \rangle^T = \sigma_e + \sum_i (\partial \sigma / \partial \mathbf{R}_i)_e \langle \mathbf{R}_i \rangle^T + \frac{1}{2} \sum_{i,j} (\partial^2 \sigma / \partial \mathbf{R}_i \partial \mathbf{R}_j)_e \langle \mathbf{R}_i \mathbf{R}_j \rangle^T + \dots \quad (4)$$

where \mathbf{R}_i are curvilinear internal displacement coordinates such as Δr_i and $\Delta \alpha_{ij}$, which are mass-independent. The isotope shift is given by,

$$\begin{aligned} \langle \sigma \rangle^T - \langle \sigma \rangle^{T'} &= \sum_i (\partial \sigma / \partial \mathbf{R}_i)_e [\langle \mathbf{R}_i \rangle - \langle \mathbf{R}_i \rangle'] (T) \\ &+ \frac{1}{2} \sum_{i,j} (\partial^2 \sigma / \partial \mathbf{R}_i \partial \mathbf{R}_j)_e [\langle \mathbf{R}_i \mathbf{R}_j \rangle - \langle \mathbf{R}_i \mathbf{R}_j \rangle'] (T) \\ &+ \dots \end{aligned} \quad (5)$$

Thus, both the temperature dependence of the shielding in the gas phase zero-pressure limit and the isotope shift contain information about the nuclear shielding surface (in the form of its derivatives at the equilibrium configuration of the molecule) and the potential energy surface (in terms of thermal averages of bond displacements and angle deformations and mean square amplitudes).

To first approximation, the series in Eq. (4) and (5) may be truncated at the linear terms.

$$\sigma_0(T) - \sigma_0(300 \text{ K}) = \sum_i (\partial \sigma / \partial \mathbf{R}_i)_e [\langle \mathbf{R}_i \rangle^T - \langle \mathbf{R}_i \rangle^{300 \text{ K}}] + \dots \quad (6)$$

$$\sigma - \sigma' = \sum_i (\partial \sigma / \partial \mathbf{R}_i)_e [\langle \mathbf{R}_i \rangle - \langle \mathbf{R}_i \rangle'] (T) + \dots \quad (7)$$

For diatomic molecules it has been shown that Eq. (6) is a very good approximation whereas Eq. (7) is not always so.³⁷ The temperature effect on bond displacement [$\langle \mathbf{R}_i \rangle^T - \langle \mathbf{R}_i \rangle^{300 \text{ K}}$] includes an important and frequently dominant rotational contribution which is

linearly dependent on T , thus making this term more important than the term containing the temperature effect on the vibrational mean square amplitudes [$\langle \mathbf{r}_i \mathbf{r}_j \rangle^T - \langle \mathbf{r}_i \mathbf{r}_j \rangle^{300}$].³⁸⁻⁴² On the other hand, the mass effect on bond displacement [$\langle \mathbf{r}_i \rangle - \langle \mathbf{r}_i \rangle'$](T) has little or no rotational contribution.⁴¹⁻⁴² In some cases, therefore, notably in the HF molecule, the contribution to the isotope shift from the [$\langle \Delta r \rangle^2 - \langle (\Delta r)^2 \rangle'$] term can be comparable to the contribution from the [$\langle \Delta r \rangle - \langle \Delta r \rangle'$] term. In the worst case, HF, they constitute roughly 1/3 and 2/3 of the observed isotope shift respectively.³⁷ In most other molecules where higher derivatives have been calculated, the contributions to the NMR isotope shift due to the $\langle \Delta r \rangle$ term has been found to dominate over all the others.^{10,37} Also, it has been shown for bent triatomic molecules H_2O , H_2S , H_2Se , O_3 , SO_2 , and SeO_2 as well as for pyramidal molecules NH_3 , PH_3 , NF_3 , and PF_3 that the mass effects on the mean bond displacement [$\langle \Delta r \rangle - \langle \Delta r \rangle'$] are much greater than that on the mean bond angle deformations [$\langle r \Delta \alpha \rangle - \langle r \Delta \alpha \rangle'$].⁴² These trends are used as the basis for interpretation of the observed temperature dependence of ^{19}F shielding in $\text{O}=\text{CF}_2$,³⁹ ^{15}N in NNO ,⁴⁰ ^{13}C in CO_2 ,⁴⁰ ^{13}C in CH_4 .⁴¹ The temperature dependence of the mean bond displacements $\langle \Delta r_i \rangle^T$ has been calculated for these molecules by Osten and Jameson using the method of Bartell,⁴⁶ in which $\langle \partial V / \partial z_i \rangle = 0$, the quantum mechanical analog of Ehrenfest's theorem, leads to coupled linear equations which relate the mean displacements $\langle \Delta r_i \rangle$ and $\langle \Delta \alpha_{ij} \rangle$ to the mean square amplitudes $\langle \Delta r_i \Delta r_j \rangle$, $\langle \Delta r_i \Delta \alpha_{ij} \rangle$, etc. The coefficients of the mean square amplitudes in these coupled equations are the quadratic and cubic force constants in the intramolecular potential V for the molecule. The method is implemented such as to include up to quadratic terms in the curvilinear relationship between $\langle \Delta r \rangle$ and the cartesian displacements.³⁹

The mass dependence of $\langle \Delta r_i \rangle$ has been determined in these molecules for $3/2/1\text{H}$, $13/12\text{C}$, $15/14\text{N}$, and $18/16\text{O}$ isotopes providing the basis for the interpretation of the observed isotope shifts. The temperature and mass dependence of $\langle \Delta r_i \rangle$ and of $\langle r \Delta \alpha_{ij} \rangle$ in the molecules H_2O , H_2S , H_2Se , O_3 , SO_2 , SeO_2 , NH_3 , PH_3 , NF_3 , and PF_3 have also been calculated by Osten and Jameson, using the same Bartell approach, for $2/1\text{H}$ and $18/16\text{O}$ isotopes. These are then used in the interpretation of the isotope shifts and temperature depen-

dence of nuclear shielding in the zero-pressure limit for some of these molecules.⁴²

The temperature dependence of $r\langle\Delta\alpha\rangle$ in the bent triatomic molecules and in NH_3 is found to be opposite that of $\langle\Delta r\rangle$. This arises from the rotational contribution to the mean bond angle deformation having a negative temperature coefficient, that is, the bond angle decreases with increasing temperature. Thus, the temperature dependence of the shielding in these bent molecules could consist of two terms of opposing sign, if the shielding derivatives $(\partial\sigma/\partial\Delta r)_\theta$ and $(\partial\sigma/\partial\Delta\alpha)_\theta$ are of the same sign. This provides a possible explanation for the unusual temperature dependence of ^{15}N shielding in NH_3 , which is also observed for ^{31}P shielding in PH_3 .

The interpretation of the temperature dependence of nuclear shielding in the zero-pressure limit using Eq. (6) allows the determination of a single parameter from the experimental curves, an empirical estimate of a shielding derivative, $(\partial\sigma/\partial\Delta r)_\theta$. Some examples of these have been reviewed.⁴⁷ The interpretation of nmr isotope shifts using Eq. (7) allows the determination of an empirical estimate of $(\partial\sigma/\partial\Delta r)_\theta$ as well, in favorable cases. Isotope shifts can be measured with much better precision than the temperature dependence of shielding in the zero-pressure limit, so that this appears to be an attractive alternative. However, since the quadratic terms not shown in Eq. (7) make significant contributions to the isotope shift in some cases (HF for example), these estimates are not necessarily superior to those obtained from the less precise temperature coefficients in the zero-pressure limit. These two sources of empirical knowledge of the shielding surface are complementary.

The ^{19}F nuclear shielding has been measured as a function of temperature in the gas phase zero-pressure limit for the following molecules: CF_2H_2 , CF_2HCl , CFHCl_2 , CF_2Cl_2 , CFCl_3 , CF_3I , CF_3CN ,⁴⁹ $\text{CF}_2=\text{CH}_2$, $\text{CF}_2=\text{CF}_2$.⁵⁰ These are shown in Table 5. The temperature coefficients of ^{19}F shielding in the fluoromethanes (the above molecules plus others previously reported, CH_3F , CF_3H , CF_4 , CF_3Cl , and CF_3Br) are found to vary systematically with the absolute ^{19}F shielding in these molecules, especially when a series of related molecules (e.g., CFH_3 , CF_2H_2 , CF_3H , CF_4) is considered. The less shielded ^{19}F nuclei have larger temperature coefficients.⁵¹ It is also found that the $^{13}/^{12}\text{C}$ -induced isotope shifts in the ^{19}F

shielding correlate with these temperature coefficients, i.e., the magnitudes are nearly linearly related. This is not surprising if Eq. (6) and (7) are valid. The dynamic factors characteristic of the C-F bond do not change drastically from one molecule to the next, and both the observed quantities are determined by $(\partial\sigma^F/\partial\Delta r_{CF})_e$. Thus, the correlation between the temperature coefficients and the absolute shielding implies a correlation between the shielding derivative and the absolute shielding.

Table 5. Temperature dependence of the ^{19}F nuclear shielding in the zero-pressure limit.⁴⁸⁻⁵⁰

Molecule	T range, K	$[\sigma_0(T) - \sigma_0(300\text{ K})]/\text{ppb} = a_1(T-300) + a_2(T-300)^2$	
		a_1	a_2
CF_2Cl_2	265-380	-9.06	
CFCl_3	310-380	-11.65	
CF_2HCl	255-380	-4.86	-1.19×10^{-2}
CFHCl_2	280-380	-5.92	
CF_2H_2	230-380	-2.89	-1.69×10^{-2}
CF_3I	237-380	-7.57	-2.12×10^{-2}
CF_3CN	300-380	-9.25	
$\text{CF}_2=\text{CF}_2$	230-350	-8.13	-2.09×10^{-2}
$\text{CF}_2=\text{CH}_2$	225-380	-4.07	-1.69×10^{-2}

C. Isotope Shifts.— A review of isotope shifts, with emphasis on $2/1\text{H}$ -induced ^{13}C shifts has appeared.⁵² In addition, isotope shifts are reported for several observed nucleus/isotope pairs.⁵³⁻⁷² We use Gombler's notation ${}^n\Delta_A(m'/m_X)$ for a shift in the observed A resonance frequency due to substitution of $m'X$ for m_X ($m' > m$) n bonds away from the observed nucleus.

$1-4\Delta^{13}\text{C}(2/1\text{H})$ values for 13 isotopomers of adamantane- d_9 show additivity and geometrical dependence of the isotope shifts.⁵³ 1Δ and 2Δ are -400 and -100 ppb respectively. The exo and respectively endo 1Δ to 4Δ effects are additive. The 3Δ and 4Δ are 0 to -55 ppb and +16.9 to -13.5 ppb respectively. The 3Δ dependence on the dihedral angle is analogous to $3J$ (Karplus-type equation) but the values of 3Δ close to 0° are considerably larger than those at

180°. In all cases the O atom is spatially close to the γ carbon in question or to a H directly bonded to it. A through-space interaction of the α H/O with the electrons surrounding the γ carbon is proposed to account for this. A through-space interaction which is partly steric and partly C-H(O) dipole- δ C electron interaction is also proposed for the $^4\Delta$ effect. The ^{13}C -induced ^{19}F shifts in fluoroadamantanes and fluorodiamantanes are reported as δ_{F} (nearer to ^{13}C) - δ_{F} (farther from ^{13}C).⁵⁷ Because isotopic substitution is in the ring system, what is observed are composite isotope effects through several paths. For the fluoroadamantanes, ($^1\Delta$ - $^3\Delta$ - $^5\Delta$) = -0.016 ppm and ($^2\Delta$ + $^6\Delta$ - $^2^4\Delta$) = -0.017 ppm. For the fluorodiamantanes, ($^2\Delta$ + $^6\Delta$ - $^3\Delta$ - $^5\Delta$) = -0.007 ppm, ($^2\Delta$ + $^6\Delta$ - $^2^5\Delta$) = -0.015, -0.016 ppm, and ($^3\Delta$ + $^5\Delta$ - $^2^4\Delta$) = -0.002, -0.007, -0.011 ppm depending on the path (correlating with the $^3\text{J}(\text{CF})$ values of +2.5, +11.0, and +10.0 Hz along the same pathway). Two- and 3-bond isotope shifts in alcohols, diols, polyols and oligosaccharides, and in protonated amines under conditions of slow hydrogen exchange have been observed.⁷⁰ $^2\Delta^{13}\text{C}(^2/^1\text{H})$ is -0.090 to -0.136 ppm for COH, -0.055 to -0.097 ppm for CNH. $^3\Delta^{13}\text{C}(^2/^1\text{H})$ is -0.010 to -0.070 ppm for CCOH. Higher degree of substitution of H by other groups on N or C leads to lower magnitudes of isotope shifts, also the more shielded the ^{13}C the smaller the magnitude of the isotope shift. The latter correlation has also been noted in ^{19}F isotope shifts.⁵¹ $^1\Delta^{31}\text{P}(^{36}/^{32}\text{S})$ = -0.0184 ppm in thiophosphate anhydrides, nearly twice $^1\Delta^{31}\text{P}(^{34}/^{32}\text{S})$ = -0.0097 ppm for terminal P=S bonds.⁶⁰ The isotope shift for bridging P-S bonds is much smaller, -0.0087 and -0.004 ppm respectively. The corresponding terminal and bridging $^1\Delta^{31}\text{P}(^{18}/^{16}\text{O})$ values are -0.0455 ppm and -0.019 ppm. The magnitudes of the S-induced isotope shifts compared with the O-induced isotope shifts can be explained by the (m'-m)/m' factors in the model discussed below.⁴⁴ $^1\Delta^{19}\text{F}(^{34}/^{32}\text{S})$ is shown to have a linear dependence on the S-F bond length in a wide variety of compounds with bond lengths varying from 1.55 Å to 1.72 Å, and isotope shifts from -0.01 to -0.07 ppm.⁵⁸ The first ^{129}Xe isotope shifts are reported: -0.52 and -0.58 ppm per ^{18}O substitution in XeO_2F_2 and XeOF_4 respectively.⁶⁴ The large magnitudes of these shifts compared to other ^{18}O -induced shifts are consistent with the previously noted dependence of the isotope shift on the chemical shift range of the observed nucleus.⁴³ In $\text{HC}\equiv\text{CH}$ the one-bond O-induced ^{13}C isotope

shift is smaller than the two-bond shift, they are -0.223 and -0.438 ppm respectively.⁵⁵ Another large two-bond shift is $2\Delta^{17}\text{O}(^{18}/^{16}\text{O}) = -0.108 \pm 0.002$ ppm in $[\text{O}=\text{U}=\text{O}]^{2+}$,⁶⁵ although this is not so unusual when the chemical shift range of ^{17}O is compared to ^{13}C . Several isotope shifts of transition metal nuclei have been observed recently.⁶¹⁻⁶³ ^{13}C -induced metal shifts have the usual sign, -0.73 ppm for ^{55}Mn in $(\text{RNC})_6\text{MnBF}_4$,⁶³ and -0.27 ppm per ^{13}C for ^{51}V in hexacarbonyl vanadate, $\text{V}(\text{}^{12}\text{CO})_6\text{-n}(\text{}^{13}\text{CO})_n^-$.⁶¹ The usual additivity is observed in the latter, the isotope shift in the ^{51}V spectrum is proportional to the number of ^{13}CO . It has been proposed that the magnitude and sign of the one-bond isotope shift in XH_4 and XO_4 depends on the atomic number Z_X as follows: with increasing Z_X in the period the isotope shift becomes increasingly negative, while with increasing Z_X in the group the isotope shift increases algebraically and even changes sign.⁶² This trend across a period can indeed be perceived when all the observed one-bond isotope shifts for a given nucleus are included, reduced by the appropriate mass factors (*vide infra*). However, in contrast to the above hypothesis, the trend down a group is similar to that across a period.

Models which consider a D atom as having different electronic properties than H atom as a substituent continue to appear.⁷³⁻⁷⁵ While these models may predict some systematic trends and stereochemical dependence of $2/^{14}\text{H}$ -induced ^{13}C isotope shifts, they necessarily invoke a breakdown of the Born-Oppenheimer approximation. That is, within the Born-Oppenheimer approximation these models would lead to no isotope shifts at all.

When substitution takes place at equivalent positions, the magnitude of the isotope shift is observed to be proportional to the number of atoms that have been substituted by isotopes. This additivity has been observed to hold within experimental error in nearly every case for one-bond as well as 2- and 3-bond isotope effects. There is also an almost (not quite) linear dependence on mass change observed in cases where more than two isotopes of the same substituent are involved, as in $^{36}/^{34}/^{32}\text{S}$. The theoretical basis for the observed additivities has been demonstrated by Osten and Jameson using the isotopomers of methane $\text{CX}_{4-\text{n}}\text{Y}_{\text{n}}$ ($\text{X}, \text{Y} = \text{H}, \text{D}, \text{T}$) and the isotopomers of linear triatomic molecules OCO , OCS , NNO ($^{13}/^{12}\text{C}$, $^{18}/^{17}/^{16}\text{O}$, $^{34}/^{32}\text{S}$, $^{15}/^{14}\text{N}$).^{41,44} In $^{12}\text{CH}_{4-\text{n}}\text{D}_{\text{n}}$ it is found

that

$$\langle \Delta r_{\text{CD}} \rangle_{\text{vib}} = d - \Delta + \delta_{\text{D}}(n), \quad (8)$$

$$\langle \Delta r_{\text{CH}} \rangle_{\text{vib}} = d + \delta_{\text{H}}(n), \quad (9)$$

where $d \equiv \langle \Delta r_{\text{CH}} \rangle_{\text{vib}}$ in $\text{CH}_4 = 2.0881 \times 10^{-2}$ Å at 300 K,

$$d - \Delta \equiv \langle \Delta r_{\text{CD}} \rangle_{\text{vib}} \text{ in } \text{CD}_4,$$

in which $\Delta = 5.5345 \times 10^{-3}$ Å at 300 K, and δ_{D} and δ_{H} are small secondary effects ($\delta \ll \Delta$) which depend on n . Thus, the sum of the vibrational contributions to the mean bond displacements is

$$\begin{aligned} \sum_{i=1}^4 \langle \Delta r_i \rangle_{\text{vib}} &= (4-n) \langle \Delta r_{\text{CH}} \rangle_{\text{vib}} + n \langle \Delta r_{\text{CD}} \rangle_{\text{vib}} \\ &= 4d - n\Delta + \delta(n) \end{aligned} \quad (10)$$

The rotational (centrifugal stretching) contribution to the mean C-H or C-D bond displacement is shown to be dependent on n but the sum of all four is invariant to n , i.e.,

$$\begin{aligned} (4-n) \langle \Delta r_{\text{CH}} \rangle_{\text{rot}} + n \langle \Delta r_{\text{CD}} \rangle_{\text{rot}} \\ = 4(5.24 \times 10^{-4} \text{ Å}) \text{ at } 300 \text{ K.} \end{aligned} \quad (11)$$

If Eq. (7) is used, the ^{13}C isotope shift between any two isotopomers can be expressed as:

$$\begin{aligned} \sigma^{\text{C}}(\text{CH}_{4-n}\text{D}_n) - \sigma^{\text{C}}(\text{CH}_{4-n'}\text{D}_{n'}) &\approx (\partial \sigma^{\text{C}} / \partial \Delta r)_e \sum_i [\langle \Delta r_i \rangle - \langle \Delta r_i \rangle'] (T) \\ &= (\partial \sigma^{\text{C}} / \partial \Delta r)_e \cdot [4d - n\Delta + \delta(n) - (4d - n'\Delta + \delta(n'))] \\ &\approx (\partial \sigma^{\text{C}} / \partial \Delta r)_e (n' - n) \Delta. \end{aligned} \quad (12)$$

This expresses the proportionality of the isotope shift to the number of substitutions at equivalent sites. The small deviations from additivity which have been observed in NH_4^+ ion, an analog of CH_4 , has been interpreted in terms of the secondary effects δ .⁴⁴ For $\text{CH}_{4-n}\text{D}_n$ ($n = 0$ to 4) the deviations from additivity are predicted to be in the ratio 0 : 3 : 4 : 3 : 0, which is the same as the observed small deviations in $\text{NH}_{4-n}\text{D}_n^+$.⁷⁶

The mass dependence of $\langle \Delta r \rangle$ in CH_4 , CD_4 , CT_4 and all isotopomers of several triatomic molecules, is found to obey the following

general relationship for a single substitution of mass m by m' :⁴⁴

$$\langle \Delta r \rangle - \langle \Delta r \rangle' = \langle \Delta r \rangle [(m' - m)/m'] f(m, m_A, \dots) \quad (13)$$

If Eq. (7) holds, then the isotope shifts will be proportional to $(m' - m)/m'$. This is shown in Fig. 1 to be nicely verified by the $m'/^{74}\text{Se}$ -induced ^{77}Se one-bond isotope shifts observed in each of four series of molecules $R_1^{77}\text{Se}^{m'}\text{Se}R_2$ ($R_1, R_2 = \text{CH}_3, \text{CF}_3$). When m'/m_X is an end atom, the complete mass dependence of $\langle \Delta r_{AX} \rangle$ upon a single substitution of mX by $^{m'}X$ is found to be well represented by⁴⁴

$$\langle \Delta r_{A^{m'}X} \rangle - \langle \Delta r_{A^mX} \rangle \approx \langle \Delta r_{A^mX} \rangle [(m' - m)/m'] [m_A/2(m_A + m)]. \quad (14)$$

For diatomic molecules this reduces to the same form as previously derived,⁴³

$$\langle \Delta r \rangle - \langle \Delta r \rangle' = \langle \Delta r \rangle (\mu' - \mu)/2\mu'. \quad (15)$$

Thus, if Eq. (7) is used, to a first approximation the one-bond isotope shift of nucleus A upon substitution of an end atom can be expressed as:⁴⁴

$$^1_{\Delta A}(m'/m_X) \approx (\partial \sigma / \partial \Delta r_{AX})_e \langle \Delta r_{A^mX} \rangle \cdot [(m' - m)/m'] [m_A/2(m_A + m)] \quad (16)$$

Thus, the least favorable isotope shifts to observe are those for a light nucleus upon substitution of a heavy one. The reasons are easily seen in Eq. (16). For light nuclei the derivative is small (reflecting the small chemical shift range), the mass factor $m_A/(m_A + m)$ is much less than 1 and so is the mass factor $(m' - m)/m'$. The largest isotope shifts are predicted for heavy nuclei upon substitution of H by D or T, where the mass factor $m_A/(m_A + m)$ is nearly 1.0 and $(m' - m)/m'$ is $1/2$ or $2/3$.

A method of estimating $\langle \Delta r_{AX} \rangle$ itself from the bond length, the masses, and the rows of the periodic table to which A and X belong, without knowledge of force fields, has been proposed by Jameson and Osten.⁴⁵ This allows the estimation of the dynamic factor in Eq. (16) and permits the electronic factor, the shielding derivative, to be estimated from an observed one-bond isotope shift. This method is based on a Morse diatomic molecule approximation for the AX bond, which is a reasonable approximation if X is an end atom. In this case,

$$\langle \Delta r \rangle_{\text{vib}} = (3a/2) \langle (\Delta r)^2 \rangle_{\text{vib}}, \quad (17)$$

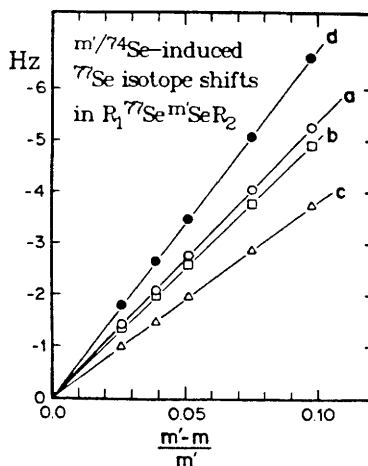


Fig.1 Effect of selenium isotopes on the ^{77}Se nuclear shielding in the diselenides $\text{R}_1^{77}\text{Se}^m\text{SeR}_2$. (a) $\text{R}_1=\text{R}_2=\text{CH}_3$; (b) $\text{R}_1=\text{R}_2=\text{CF}_3$; (c) $\text{R}_1=\text{CF}_3$, $\text{R}_2=\text{CH}_3$; (d) $\text{R}_1=\text{CH}_3$, $\text{R}_2=\text{CF}_3$ from the experimental results in W. Gombler, *J. Magn. Reson.*, 1982, 53, 69.

where a is the Morse parameter. The mean bond displacement in a diatomic molecule is reasonably well-represented by⁴⁵

$$\langle \Delta r \rangle_{\text{vib}} \approx 19.35 \times 10^{-3} \mu^{-1/2} 10^{-D}, \quad (18)$$

where μ is the reduced mass of AX in amu, and

$$D \equiv (r_e - a_3)/b_3 - 3(r_e - a_2)/2b_2, \quad (19)$$

in which a_2 , b_2 , a_3 , and b_3 are constants tabulated by Herschbach and Laurie for different rows of the periodic table.⁷⁷ For the AX bond in a polyatomic molecule,

$$\langle \Delta r \rangle_{\text{vib}} = 22 \times 10^{-3} \mu^{-1/2} 10^{-D}. \quad (20)$$

The constant factor is modified somewhat to fit results of calculations of $\langle \Delta r \rangle$ in several polyatomic molecules.

Because of the relationship Eq. (17) for a diatomic molecule, it is relatively easy to include quadratic terms in Eq. (16) for a diatomic molecule:

$${}^1\Delta A(m'/m_X) = [(\partial\sigma/\partial\Delta r_{AX})_e + (1/3a)(\partial^2\sigma/\partial\Delta r_{AX}^2)] \cdot \langle\Delta r_{AX}^m\rangle \cdot [(m'-m)/m'] [m_A/2(m_A+m)]. \quad (21)$$

For polyatomic molecules there are other second derivatives besides the one for bond stretch; nevertheless, in the context of the approximations used in Eq. (16), Eq. (21) could just as well be applied to an isotope shift upon single substitution in a polyatomic molecule. The Morse parameter a is of the order of 2 \AA^{-1} and is likewise expressible in terms of the Herschbach-Laurie parameters. Using Eq. (19) or (20) enables us to estimate the electronic factor $[(\partial\sigma/\partial\Delta r)_e + (1/3a)(\partial^2\sigma/\partial\Delta r^2)_e]$ from the observed isotope shift knowing only the bond length r_e , the masses, and the rows of the periodic table to which the atoms A and X belong.⁴⁵ Since the calculations on bent triatomics and pyramidal molecules show that the mass dependence of the bond angle is small compared to that of the bond length, Eq. (21) can even be applied to these systems, so long as the mass substitution is at an end atom.⁴² It is convenient to define a "reduced isotope shift" which takes into account the explicit mass factors in Eq. (21):⁴⁵

$$\Delta^R(A,X) \equiv {}^1\Delta A(m'/m_X) \{[(m'-m)/m'] [m_A/2(m_A+m)]\}^{-1} \quad (22)$$

Although Δ^R is not completely mass-independent ($\langle\Delta r_{AX}\rangle$ itself is mass-dependent), the reduced isotope shift does allow the isotope shifts of different nuclei in a variety of environments to be compared with one another. The rovibrational correction to the nuclear shielding of A in an AX_n molecule can be estimated from the isotope shift. For a diatomic molecule this is given by

$$\sigma_0(T) - \sigma_e \approx (\partial\sigma/\partial\Delta r)_e \langle\Delta r\rangle + \frac{1}{2} (\partial^2\sigma/\partial\Delta r^2)_e \langle(\Delta r)^2\rangle \quad (23)$$

which is the same as the right side of Eq. (21) except for the mass factors. Therefore the rovibrational correction to nuclear shielding for a diatomic molecule is given by the reduced isotope shift itself:

$$\sigma_0^A(T) - \sigma_e^A = \Delta^R(A,X). \quad (24)$$

For an AX_n molecule the rovibrational correction to the nuclear shielding of A is estimated by

$$\sigma_0^A(T) - \sigma_E^A \approx n\Delta^R(A,X). \quad (25)$$

This provides a simple, though approximate, correction to experimental shielding values before comparison with theoretically calculated σ_E values.

D. Intermolecular Effects.— Theoretical calculations (using Ditchfield's GIAO FPT method with a 4-31 basis set) of intermolecular effects on nuclear shielding in hydrogen-bonded systems have been reported.⁷⁸⁻⁸² The calculations of ^1H shielding in H_2O , $(\text{H}_2\text{O})_2$, $(\text{H}_2\text{O})_3$, $(\text{H}_2\text{O})_5$ using the ice geometry show the effects of secondary and primary hydrogen bonding in ice. The dimer only contains the primary effects (11.28 ppm increase in the shielding anisotropy and 2.81 ppm decrease in the isotropic shielding), the trimer and pentamer show the effect of remote water molecules (a further 5.18 ppm increase in the anisotropy and 1.34 ppm decrease in the isotropic shielding).⁷⁸ Shielding calculations are reported for the following clusters, using the method reported in Vol. 14 of this series:⁸³ $\text{H}_2\text{CO} \cdot (\text{H}_2\text{O})_2$, $\text{HC(O)NH}_2 \cdot (\text{H}_2\text{O})_4$, imidazole $\cdot (\text{H}_2\text{O})_2$, $(\text{C}_2\text{H}_4)_2$, $(\text{H}_2\text{CO})_2$.⁷⁹ The results show that for C, O, and N the largest contribution to the shift due to hydration is the "polarization shift", which is especially large for the O atom directly involved in the hydrogen bonds. Comparison with experiment is not so straightforward. For C_2H_4 , density-dependent gas-phase data are available; however, these calculations do not include dispersion effects nor do they average over all orientations weighted by the intermolecular potential. The sign of the ^{13}C shift in going from C_2H_4 to $(\text{C}_2\text{H}_4)_2$ is strongly basis-set-dependent, so no conclusion can be drawn from the calculations. The sign of the ^1H shift is the same as that which is normally observed with increasing density in the gas phase and appears to be dominated by the geometric contribution. The effects of hydration on C, O, and N shielding in H_2CO and HC(O)NH_2 are attributed to polarization shifts. For hydrated formamide the calculations on the $\text{HC(O)NH}_2 \cdot (\text{H}_2\text{O})_{10}$ cluster yield the following shielding changes relative to the unhydrated molecule: N -15.65 ppm, C -4.94 ppm, O 203.38 ppm, that is, N and C are deshielded whereas O becomes more shielded by 203 ppm!⁸⁰ It would be useful to compare absolute shieldings calculated for the hydrated molecule with experimental values for an aqueous solution of formamide. The attached ^{13}C nuclei in C_2H_2 , C_2H_4 , and C_2H_6 are

deshielded upon complexation with Ni, whereas the other carbon shifts in the opposite direction, according to model calculations of ^{13}C shielding tensors in these coordinated hydrocarbons.⁸⁴

A gauge of the reliability of the conclusions based on the above theoretical results could have been provided by citing some experimental shielding values in the literature. For ^{13}C , ^{15}N , and ^{17}O , measured chemical shifts can be converted into absolute shielding by making the connection with the liquid reference used and the primary reference. The latter are $\sigma(^{13}\text{C in CD}) = 3.20 \pm 0.27$ ppm,¹⁶ $\sigma(^{15}\text{N in NH}_3) = 264.54 \pm 0.2$ ppm⁸⁵ and $\sigma(^{17}\text{O in CD}) = -42.3 \pm 17.2$ ppm.⁹ On these absolute shielding scales the usual liquid reference shieldings at room temperature are $\sigma(^{13}\text{C in TMS, cyl}) = 185.4$ ppm,¹⁵ $\sigma(^{15}\text{N in CH}_3\text{NO}_2, \text{ cyl}) = -135.8$ ppm⁸⁵ and $\sigma(^{17}\text{O in H}_2\text{O, cyl}) = 307.9$ ppm.⁹ For ^1H the absolute shielding scale is based on the H atom⁸⁶ and on this scale the absolute $\sigma(^1\text{H in H}_2\text{O, sph}) = 25.790 \pm 0.014$ ppm.⁸⁶ The experimental absolute shielding can then be obtained from the measured chemical shifts δ , by $\delta = \sigma(\text{ref}) - \sigma(\text{sample})$. This reporter recommends that comparisons with experimental shieldings be made in reporting any theoretical calculations. There will, of course, be effects of rotational-vibrational averaging and intermolecular interactions included in the experimental values, but these can be estimated from the magnitudes and signs of these effects which have been reported in previous volumes of this series.

Gas-phase NMR studies of hydrogen-bonding association in the $(\text{CH}_3)_2\text{O} \cdot \text{HCl}$ system provide an experimental value for the proton shielding change on hydrogen-bond formation (2.510 ppm) in a system sufficiently simple for theoretical calculations.⁸⁷ This shift may be interpreted as the difference in shielding between the proton in free HCl and in the $(\text{CH}_3)_2\text{O} \cdot \text{HCl}$, unlike shifts measured in condensed phases. The effects of van der Waals interactions on nuclear shielding can be studied by measuring the density dependent shifts in the dilute gas phase. These interactions lead to deshielding, i.e., the second virial coefficient of nuclear shielding is negative. The density dependence of ^{19}F shielding in the molecules shown in Table 6 correlates with the polarizability, except where electric moments give additional contributions to the second virial coefficients of shielding.^{48-50,88} The gas-to-liquid shift data for these molecules are also reported as a function of temperature

and are found to be consistent with the density dependence in the dilute gas phase, with additional many-body shielding effects.

Table 6 Second virial coefficient of ^{19}F nuclear shielding in the pure dilute gas,^{48-50,88} and molecular polarizability.⁹⁰

Gas	T range, K	$\sigma_1 = \lim_{\rho \rightarrow 0} (\partial\sigma/\partial\rho)_T$, ppb amagat ⁻¹	$\alpha/10^{-25}\text{cm}^3$
CFH_3	280-380	-13.7 ± 1.8	$2.6 \times 10^{-2}(T-300)$ 26.0
CF_2H_2	300-380	-4.8 ± 1.1	26.5
CF_3H	240-380	-6.8 ± 0.7	$4.0 \times 10^{-2}(T-300)$ 26.9
CF_4	270-410	-8.6 ± 0.3	27.3
CF_2HCl	300-380	-13.6 ± 0.9	45.4
CF_3Cl	220-380	-15.7 ± 1.8	$3.6 \times 10^{-2}(T-300)$ 45.8
CF_3Br	300-380	-21.1 ± 0.6	$5.3 \times 10^{-2}(T-300)$ 56.6
CFHCl_2	350-380	-21.6 ± 1.4	63.9
CF_2Cl_2	330-380	-16.8 ± 1.7	$6.7 \times 10^{-3}(T-300)$ 64.3
CF_3I	340-380	-24.0 ± 2.1	$1.4 \times 10^{-1}(T-300)$ 74.4
CFCl_3	350-380	-15.8 ± 1.7	82.8
CF_3CN	300-380	-17.2 ± 1.0	$4.5 \times 10^{-2}(T-300)$
$\text{CF}_2=\text{CH}_2$	290-380	-12.9 ± 0.6	40.8
$\text{CF}_2=\text{CF}_2$	270-350	-14.8 ± 2.0	$5.2 \times 10^{-2}(T-300)$ 41.7

In $\text{CF}_2=\text{CH}_2$, a combination of the recent ^{19}F shielding data in the dilute gas and in the liquid⁵⁰ with the previous data for intermediate densities⁸⁹ shows a nice smooth curve of ^{19}F shielding vs. density from the zero-pressure limit all the way to the 400-amagat liquid. Such a comparison is made possible by the insignificant (within experimental error) temperature dependence of the second virial coefficient of nuclear shielding in this system. The many-body effects which become important at high densities appear to be opposite in sign to the two-body effects. A fit to a quadratic function of (density/amagat) gives $(\sigma - \sigma_0)/\text{ppm} = -0.0154\rho + 4.401 \times 10^{-6} \rho^2$.

In the $\text{F}_2=\text{CFX}$ molecule there are 3 inequivalent nuclei which are at different distances from the center of mass of the molecule: F_{trans} , F_{cis} , F_{gem} (labeled by their positions relative to the substituent X). When $\text{X}=\text{H}$, F_{trans} is closest to the center of mass, followed by F_{cis} and F_{gem} . When $\text{X} = \text{Cl}, \text{Br}, \text{or I}$, F_{trans} is

farthest from the center of mass followed by F_{cis} and F_{gem} . The σ_1 values are reported for these 12 fluorine sites.⁸⁸ It is shown that the σ_1 for these 3 sites in each molecule can be interpreted in terms of the nuclear site effect.⁸⁸ In this model, the distance of the observed nucleus from the center of mass of the molecule can be taken into account by a multiplicative factor (the site factor s) which can be calculated from the geometry of the molecule and the characteristic distance parameter r_0 of the potential.⁹¹ According to this model, the 3 nuclear probes in the molecule will exhibit σ_1 values which are related to each other in the same manner as the site factors. This is based on two assumptions, the dominance of the dispersion contribution and a constant parameter B for the C-F bond of all 3 sites in the RBB model.⁹² Indeed it is found that for $X = Cl, Br, I$, the plots of experimental σ_1 vs s give excellent straight lines. The correlation is not nearly so good for $X=H$, where it is not unexpected that the 3 C-F bonds could have different B parameters since F_{trans} and F_{gem} differ in shielding by 107 ppm!⁹³

The same nuclear site effect model accounts for the observed density dependence of the isotope shift $\sigma^D(D_2) - \sigma^D(HD)$. The greater magnitude of σ_1 in D_2 compared to σ_1 in HD is due to the larger site factor for the more exposed D nuclei in D_2 ($r_e/2$ from the center of mass) compared to HD (the D is $r_e/3$ from the center of mass).⁸⁸ Thus, the density dependence observed by Beckett and Carr,⁹⁴ $-(0.059 \pm 0.026) \times 10^{-4}$ ppm amagat⁻¹, is reproduced by the model which gives a value equal to -0.049×10^{-4} ppm amagat⁻¹.

E. Absolute Shielding Scales.- The ^{17}O and the ^{33}S absolute shielding scales have recently been determined.^{9,95} Based on the molecular beam value of the spin-rotation constant for ^{17}O in CO the ^{17}O absolute shielding in CO is -42.3 ± 17.2 ppm. The ^{17}O shielding in several molecules in the gas phase is simultaneously obtained. The results are shown in Table 7. The ^{33}S absolute shielding scale is based on $\sigma(^{33}S$ in OCS) and the ^{33}S absolute shielding of other molecules based on this are also shown in Table 7.⁹⁵ Several additions to the ^{19}F shielding scale in the form of ^{19}F data in the zero-pressure limit have been reported.⁹³ There are also 1H shift data in the gaseous alcohols in the zero-pressure limit.⁹⁶ Unfortunately the reference used is internal TMS gas which

has not yet been related to ^1H in liquid H_2O at 298 K.

Table 7 Absolute shielding scale for ^{17}O based on $\sigma(\text{CO}) = -42.3 \pm 17.2 \text{ ppm}^9$ and ^{33}S based on $\sigma(\text{OCS}) = 843 \pm 12 \text{ ppm}^{95}$

$\sigma(^{17}\text{O})/\text{ppm}$		$\sigma(^{33}\text{S})/\text{ppm}^a$	
$\text{H}_2\text{O}(\text{gas})$	344.0	$\text{OCS}(\text{beam})$	843
$\text{H}_2\text{O}(\text{liq.}, 293 \text{ K})$	307.9	OCS	843
$\text{CO}_2(\text{gas})$	243.4	H_2S	752
$\text{NNO}(\text{gas})$	200.5	CH_3SH	707
$\text{OCS}(\text{gas})$	107.9	CS_2	581
$\text{CO}(\text{gas})$	-42.3	SF_6	426
$\text{OF}_2(\text{gas})$	-473.1	SO_2F_2	290
		$(\text{NH}_4)_2\text{SO}_4$ 4.2m, aq.	249
		$\text{SOCl}_2(223 \text{ K})$	25
		SO_2	-126

^aFor the neat liquid at 295 K unless otherwise specified, neglecting the OCS gas-to-liquid shift which is estimated to be $\sim -5 \text{ ppm}$.

References

- 1 H. Nakatsuji, K. Kanda, K. Endo, and T. Yonezawa, *J. Am. Chem. Soc.*, 1984, **106**, 4653.
- 2 K. Kanda, H. Nakatsuji, and T. Yonezawa, *J. Am. Chem. Soc.*, 1984, **106**, 5888.
- 3 A. D. Buckingham and S.M. Malm, *Mol. Phys.*, 1971, **22**, 1127.
- 4 J. C. Facelli, A. M. Orendt, D. M. Grant, and J. Michl, *Chem. Phys. Lett.*, 1984, **112**, 147.
- 5 M. Iwai and A. Saika, *Chem. Phys. Lett.*, 1983, **95**, 596.
- 6 C. M. Rohlifing, L. C. Allen, and R. Ditchfield, *Chem. Phys.*, 1984, **87**, 9.
- 7 V. Galasso, *Chem. Phys. Lett.*, 1984, **108**, 435.
- 8 H. Fukui, K. Miura, H. Yamasaki, and T. Nosaka, *J. Chem. Phys.*, 1985, **82**, 1410.
- 9 R. E. Wasylishen, S. Mooibroek, and J. B. Macdonald, *J. Chem. Phys.*, 1984, **81**, 1057.
- 10 P. W. Fowler and W. T. Raynes, *Mol. Phys.*, 1981, **43**, 65; P. W. Fowler, G. Riley, and W. T. Raynes, *Mol. Phys.*, 1981, **42**, 1463.
- 11 R. Bramley, M. Brorson, A. M. Sargeson, and C. E. Schaffer, *J. Am. Chem. Soc.*, 1985, **107**, 2780.
- 12 T. Yamanobe, I. Ando, H. Saito, R. Tabeta, A. Shoji, and T. Ozaki, *Bull. Chem. Soc. Jpn.*, 1985, **58**, 23.
- 13 B. N. Chernyshov, G. P. Shchetinina, V. L. Pershin, and E. G. Ippolitov, *Koord. Khim.*, 1984, **10**, 171.
- 14 A. J. Beeler, A. M. Orendt, D. M. Grant, P. W. Cutts, J. Michl, K. W. Zilm, J. W. Downing, J. C. Facelli, M. S. Schindler, and W. Kutzelnigg, *J. Am. Chem. Soc.*, 1984, **106**, 7672.
- 15 J. Mason, *J. Chem. Soc. Perkin Trans. 2*, 1976, 1671.

- 16 D. B. Neumann and J. W. Moskowitz, J. Chem. Phys., 1969, 50, 2216; I. Ozier, L. M. Crapo and N. F. Ramsey, J. Chem. Phys., 1968, 49, 2314.
- 17 M. I. Burger, J. Phys. Chem., 1984, 88, 4929.
- 18 G. Dombi, P. Diehl, J. Lounila, and R. Wasser, Org. Magn. Reson., 1984, 22, 573.
- 19 B. M. Fung and C. F. Kong, J. Am. Chem. Soc., 1984, 106, 6193.
- 20 A. Manenschijn, M. J. Quijvestijn, J. Smidt, R. A. Wind, C. S. Yannoni, and T. C. Clark, Chem. Phys. Lett., 1984, 112, 99.
- 21 A. Naito and C. A. McDowell, J. Chem. Phys., 1984, 81, 4795.
- 22 W. S. Veeman, Prog. Nucl. Magn. Reson. Spectrosc., 1984, 16, 193.
- 23 G. S. Harbison, L. W. Jelinski, R. E. Stark, D. A. Torchia, J. Herzfeld, and R. G. Griffin, J. Magn. Reson., 1984, 60, 79.
- 24 E. Oldfield, M. A. Keniry, S. Shinoda, S. Schramm, T. L. Brown, and H. S. Gutowsky, J. Chem. Soc. Chem. Commun., 1985, 791.
- 25 Y. Yoshioka, N. Nakamura, and H. Chihara, Z. Naturforsch. A, 1985, 40, 137.
- 26 Q. Z. Guo, R. E. Sears, and R. D. Campbell, J. Chem. Phys., 1984, 81, 5214.
- 27 R. Grosescu and U. Haeblerlen, Z. Naturforsch. A, 1985, 40, 283.
- 28 N. Weiden and H. Rager, Z. Naturforsch. A, 1985, 40, 126.
- 29 T. M. Duncan and D. C. Douglass, Chem. Phys., 1984, 87, 339.
- 30 B. R. Appleman and B. P. Dailey in Advances in Magnetic Resonance, J. S. Waugh, ed. Academic Press, New York, 1974, Vol. 7, 231.
- 31 T. D. Gierke and W. H. Flygare, J. Am. Chem. Soc., 1972, 94, 7277; P. B. Davies, R. M. Neumann, S. C. Wofsy, and W. Klemperer, J. Chem. Phys., 1971, 55, 3564.
- 32 A. Naito, D. L. Sastry, and C. A. McDowell, Chem. Phys. Lett., 1985, 115, 19.
- 33 S. Ganapathy, V. P. Chacko, and R. G. Bryant, J. Chem. Phys., 1984, 81, 661.
- 34 R. S. Honkonen and P. D. Ellis, J. Am. Chem. Soc., 1984, 106, 5488.
- 35 V. W. Miner and J. H. Prestegard, J. Am. Chem. Soc., 1985, 107, 2177.
- 36 R. K. Harris, K. J. Packer, and P. Reams, Chem. Phys. Lett., 1985, 115, 16.
- 37 R. Ditchfield, Chem. Phys., 1981, 63, 185.
- 38 C. J. Jameson, J. Chem. Phys., 1977, 66, 4977.
- 39 C. J. Jameson and H. J. Osten, J. Chem. Phys., 1984, 81, 4915.
- 40 C. J. Jameson and H. J. Osten, J. Chem. Phys., 1984, 81, 2556.
- 41 H. J. Osten and C. J. Jameson, J. Chem. Phys., 1984, 81, 4288.
- 42 H. J. Osten and C. J. Jameson, J. Chem. Phys., 1985, 82, 4595.
- 43 C. J. Jameson, J. Chem. Phys., 1977, 66, 4983.
- 44 C. J. Jameson and H. J. Osten, J. Chem. Phys., 1984, 81, 4293.
- 45 C. J. Jameson and H. J. Osten, J. Chem. Phys., 1984, 81, 4300.
- 46 L. S. Bartell, J. Chem. Phys., 1963, 38, 1827; 1979, 70, 4581 and references cited therein.
- 47 C. J. Jameson, Bull. Magn. Reson., 1980, 3, 3.
- 48 C. J. Jameson, A. K. Jameson, and D. Oppusunggu, J. Chem. Phys., 1984, 81, 85.
- 49 C. J. Jameson and A. K. Jameson, J. Chem. Phys., 1984, 81, 1198.
- 50 C. J. Jameson, A. K. Jameson, and D. Oppusunggu, J. Chem. Phys., 1984, 81, 2571.
- 51 C. J. Jameson, Mol. Phys., 1985, 54, 73.
- 52 D. A. Forsyth in Isotopes in Organic Chemistry, 1984, 6, 1.

- 53 Z. Majerski, M. Zuanic, and B. Metelko, J. Am. Chem. Soc., 1985, 107, 1721.
- 54 J. R. Everett, J. Chem. Soc. Perkin Trans. 2, 1984, 1151.
- 55 Yu. N. Luzikov and N. M. Sergeyev, J. Magn. Reson., 1984, 60, 177.
- 56 R. Bar, Y. Sasson, and J. Blum, Org. Magn. Reson., 1984, 22, 565.
- 57 G. A. Olah, J. G. Shih, V. V. Krishnamurthy, and B. P. Singh, J. Am. Chem. Soc., 1984, 106, 4492.
- 58 W. Gombler, Z. Naturforsch. B, 1985, 40, 782.
- 59 P. B. Kay and S. Trippett, J. Chem. Soc. Chem. Commun., 1985, 135.
- 60 C. Roeske, P. Paneth, M. H. O'Leary, and W. Reimschuessel, J. Am. Chem. Soc., 1985, 107, 1409.
- 61 K. Ihmels, D. Rehder, and V. Pank, Inorg. Chim. Acta, 1985, 96, L69.
- 62 V. P. Tarasov, V. I. Privalov, Yu. A. Buslaev, and U. Eichhoff, Z. Naturforsch. B, 1984, 39, 1230.
- 63 R. M. Nielson and S. Wherland, Inorg. Chem., 1984, 23, 3265.
- 64 G. A. Schumacher and G. J. Schrobilgen, Inorg. Chem., 1984, 23, 2923.
- 65 W. S. Jung, Y. Ikeda, H. Tomiyasu, and H. Fukutomi, Bull. Chem. Soc. Jpn., 1984, 57, 2317.
- 66 D. A. Forsyth, J. H. Botkin, and V. M. Osterman, J. Am. Chem. Soc., 1984, 106, 7663.
- 67 R. Aydin, J. R. Wesener, H. Günther, R. L. Santillan, M. E. Garibay, and P. Joseph-Nathan, J. Org. Chem., 1984, 49, 3845.
- 68 V. E. U. Costa and P. R. Seidl, Actual. Fis.-Quim. Org. Conf., 2nd, 1983, 135.
- 69 A. Lycka and P. E. Hansen, Org. Magn. Reson., 1984, 22, 569.
- 70 J. Reuben, J. Am. Chem. Soc., 1985, 107, 1433, 1747, 1756.
- 71 J. M. Risley, R. L. Van Etten, C. Uncuta, and A. T. Balaban, J. Am. Chem. Soc., 1984, 106, 7836.
- 72 W. Adcock and V. S. Iyer, Tetrahedron Lett., 1984, 25, 5209.
- 73 J. R. Wesener, D. Moskau, and H. Gunther, Tetrahedron Lett., 1985, 26, 1491.
- 74 H. Kunzer and S. Berger, Tetrahedron Lett., 1984, 25, 5019.
- 75 H. Kunzer and S. Berger, J. Am. Chem. Soc., 1985, 107, 2804.
- 76 R. E. Wasylshen and J. O. Friedrich, J. Chem. Phys., 1984, 80, 585.
- 77 D. R. Herschbach and V. W. Laurie, J. Chem. Phys., 1961, 35, 458.
- 78 J. F. Hinton and D. L. Bennett, Chem. Phys. Lett., 1985, 116, 292.
- 79 S. Ferchiou and C. Giessner-Prettre, J. Magn. Reson., 1985, 61, 262.
- 80 C. Giessner-Prettre and A. Pullman, Chem. Phys. Lett., 1985, 114, 258.
- 81 C. Giessner-Prettre, J. Biomol. Struct. Dyn., 1984, 2, 233.
- 82 C. Giessner-Prettre, J. Langlet, and F. Caron, J. Theor. Biol., 1984, 107, 211.
- 83 C. Giessner-Prettre and S. Ferchiou, J. Magn. Reson., 1983, 55, 64.
- 84 E. Bauwe, G. Rasch and T. Weller, Z. Chem., 1984, 24, 26.
- 85 C. J. Jameson, A. K. Jameson, D. Oppusunggu, S. Wille, P. M. Burrell, and J. Mason, J. Chem. Phys., 1981, 74, 81.
- 86 W. D. Phillips, W. E. Cooke, and D. Kleppner, Phys. Rev. Lett., 1975, 15, 1619; T. Myint, D. Kleppner, N. F. Ramsey, and H. G. Robinson, Phys. Rev. Lett., 1966, 17, 405; P. F. Winkler, D.

- Kleppner, T. Myint and F. G. Walther, Phys. Rev. A, 1972, 5, 83.
- 87 S. H. Bauer, T. Yamazaki, K. I. Lazaar, and N. S. Chiu, J. Am. Chem. Soc., 1985, 107, 743.
- 88 C. J. Jameson, A. K. Jameson, and D. Oppusunggu, J. Chem. Phys., 1984, 81, 2313.
- 89 W. H. Wisman in Magnetic Resonance and Radiofrequency Spectroscopy, Proceedings of the 15th Colloque Ampere 1968, ed. P. Auerbuck (North-Holland, Amsterdam, 1969) 255.
- 90 J. A. Beran and L. Kevan, J. Phys. Chem., 1969, 73, 3860.
- 91 F. H. Rummens, W. T. Raynes, and H. J. Bernstein, J. Phys. Chem., 1968, 72, 2111.
- 92 W. T. Raynes, A. D. Buckingham, and H. J. Bernstein, J. Chem. Phys., 1962, 36, 3481.
- 93 C. J. Jameson, A. K. Jameson, and J. Honarbakhsh, J. Chem. Phys., 1984, 81, 5266.
- 94 J. R. Beckett and H. Y. Carr, Phys. Rev. A, 1981, 24, 144.
- 95 J. P. Chauvel and N. S. True, Chem. Phys., 1985, 95, 435.
- 96 R. E. Wasylishen, C. Connor, and J. O. Friedrich, Can. J. Chem., 1984, 62, 981.